PLOS ONE

RESEARCH ARTICLE

A strontium isoscape for the Conchucos region of highland Peru and its application to Andean archaeology

Eden Washburn[1]*, Jason Nesbitt[2], Bebel Ibarra[2], Lars Fehren-Schmitz[1], Vicky M. Oelze[1]

1 Department of Anthropology, University of California Santa Cruz, Santa Cruz, California, United States of America, **2** Department of Anthropology, Tulane University, New Orleans, Louisiana, United States of America

* ewashbur@ucsc.edu

OPEN ACCESS

Citation: Washburn E, Nesbitt J, Ibarra B, Fehren-Schmitz L, Oelze VM (2021) A strontium isoscape for the Conchucos region of highland Peru and its application to Andean archaeology. PLoS ONE 16(3): e0248209. https://doi.org/10.1371/journal.pone.0248209

Editor: David Caramelli, University of Florence, ITALY

Received: March 20, 2020

Accepted: December 12, 2020

Published: March 30, 2021

Data Availability Statement: All relevant data are within the manuscript.

Funding: EW - This research was funded by the National Science Foundation (NSF – 1842447) https://www.nsf.gov/publications/pub_summ.jsp?ods_key=nsf08564 The funders had no role in study design, data collection and analysis, decision to publish, or preparation of the manuscript.

Competing interests: The authors have declared that no competing interests exist.

Abstract

Strontium isotope ($^{87}Sr/^{86}Sr$) analysis of human skeletal remains is an important method in archaeology to examine past human mobility and landscape use. $^{87}Sr/^{86}Sr$ signatures of a given location are largely determined by the underlying bedrock, and these geology specific isotope signatures are incorporated into skeletal tissue through food and water, often permitting the differentiation of local and non-local individuals in past human populations. This study presents the results of a systematic survey of modern flora and fauna (n = 100) from 14 locations to map the bioavailable $^{87}Sr/^{86}Sr$ signatures of the Conchucos region, an area where the extent of geologic variability was previously unknown. We illustrate the necessity to examine the variation in $^{87}Sr/^{86}Sr$ values of the different geological formations available to human land use to document the range of possible local $^{87}Sr/^{86}Sr$ values. Within the Conchucos region we found significant variation in environmental $^{87}Sr/^{86}Sr$ values (0.7078–0.7214). The resulting isoscape represents the largest regionally specific bioavailable $^{87}Sr/^{86}Sr$ map (3,840 km^2) to date for the Andes, and will serve as a baseline for future archaeological studies of human mobility in this part of the Peruvian highlands.

Introduction

The study of mobility and migration are important topics in contemporary archaeology [1]. While human mobility can be studied using a variety of archaeological indicators, recent years have witnessed a marked increase in investigations that employ isotopic analyses of human remains to study ancient population movements [2–11]. Molecular methods enable researchers to focus primarily on the individual [12–16], and can elucidate aspects of human behavior such as mobility and landscape utilization that are otherwise difficult to observe [15]. Because strontium has the unique ability to substitute for calcium (Ca) in the hydroxyapatite of bone and tooth enamel, the use of strontium isotopes ($^{87}Sr/^{86}Sr$) analysis in skeletal remains can provide insight into past human and other animal movement throughout a landscape. When locally available nutrients are consumed, $^{87}Sr/^{86}Sr$ values in an organism reflect the

bioavailable (i.e., only the strontium which makes its way into the food chain; see further discussion below) signature of the immediate geological location in which an individual lived. Nevertheless, the use of $^{87}Sr/^{86}Sr$ isotope analysis to identify non-local individuals and their potential place of origin, relies on an accurate characterization of local $^{87}Sr/^{86}Sr$ ranges, either through statistical spatial modeling or by testing modern/archaeological proxy materials to establish local baselines.

In the Andes, $^{87}Sr/^{86}Sr$ isotope analysis has been used to address a wide range of fundamentally important questions surrounding human life and interaction [17–52]. Significant variation in the geology of the Andes makes the use of strontium isotopic analysis a useful tool in determining "local" vs "non-local" inhabitants of an archaeological site [15, 45, 53]. The Andes mountains are composed of many folded geological layers [54–56] that generally run in parallel from north to south and these geological formations can be relatively narrow and stacked close together. As a result, inhabitants of a specific archaeological site may have encountered (or frequented) multiple geological formations, thus making the identification of potential migrants more challenging. For example, the physical location of an archaeological site may not have been located in the same geological formation in which food was cultivated or herding and hunting was conducted.

In regions where the extent of geologic variation and the range of $^{87}Sr/^{86}Sr$ values are known, $^{87}Sr/^{86}Sr$ analysis can be used to track mobility and illuminate processes of interaction. In Peru, the majority of $^{87}Sr/^{86}Sr$ isotope studies have been situated along the Pacific coast, in the southern Andes and/or west of the Cordillera Blanca. The limited number of $^{87}Sr/^{86}Sr$ studies within the highland valley systems of the north central Andes have resulted in an underestimation of the geologic complexity throughout the region. Here we add to the growing body of $^{87}Sr/^{86}Sr$ studies in the Andes, and present the first regional map of the variation in bioavailable $^{87}Sr/^{86}Sr$ values of the Conchucos region of highland Ancash (Fig 1), a region with a rich archaeological history [57]. Our study also raises questions related to what may constitute isotope-based determinations of local and non-local populations in Andean archaeology.

Background

Strontium geochemistry

The trace element strontium (Sr) is found in extremely low concentrations in bedrock, groundwater, soil, plants, and animals. Sr is composed of different percentages of the following four stable isotopes: ^{84}Sr (~0.56%), ^{86}Sr (~9.87%), ^{87}Sr (~7.04%) and ^{88}Sr (~82.53%) [74, 75]. Of these four isotopes, ^{87}Sr is radiogenic and formed over time by the radioactive decay of rubidium (^{87}Rb) in the bedrock, which has a half-life of ~4.88 x 10^{10} years. As a result, specific concentrations of ^{87}Sr in the environment are a result of a bedrock's age and Rb content [58–60]. Sr enters the biosphere through uptake from the substrate by plants and cycles through food webs, into for example, the tissues of both animals and humans.

However, not all Sr in bedrock is uniformly weathered into the soil and water [15, 61, 62]. Various minerals found within a single bedrock unit can have considerable variability in their $^{87}Sr/^{86}Sr$ values. For example, granite can have two feldspars with radically differing $^{87}Sr/^{86}Sr$ values (plagioclase and potassium feldspars) depending on which section is measured [15]. As such, biologically available $^{87}Sr/^{86}Sr$, which is soluble and is taken up by biotic agents, can substantially differ in its values between the lithosphere and the biosphere [12, 15, 63, 64]. As a result, direct bedrock $^{87}Sr/^{86}Sr$ measurements typically conducted for geological dating studies [65–70] are not necessarily accurate for applications in archaeological science. Besides Sr deriving from the weathering of local bedrock, atmospheric and surface sources, such as

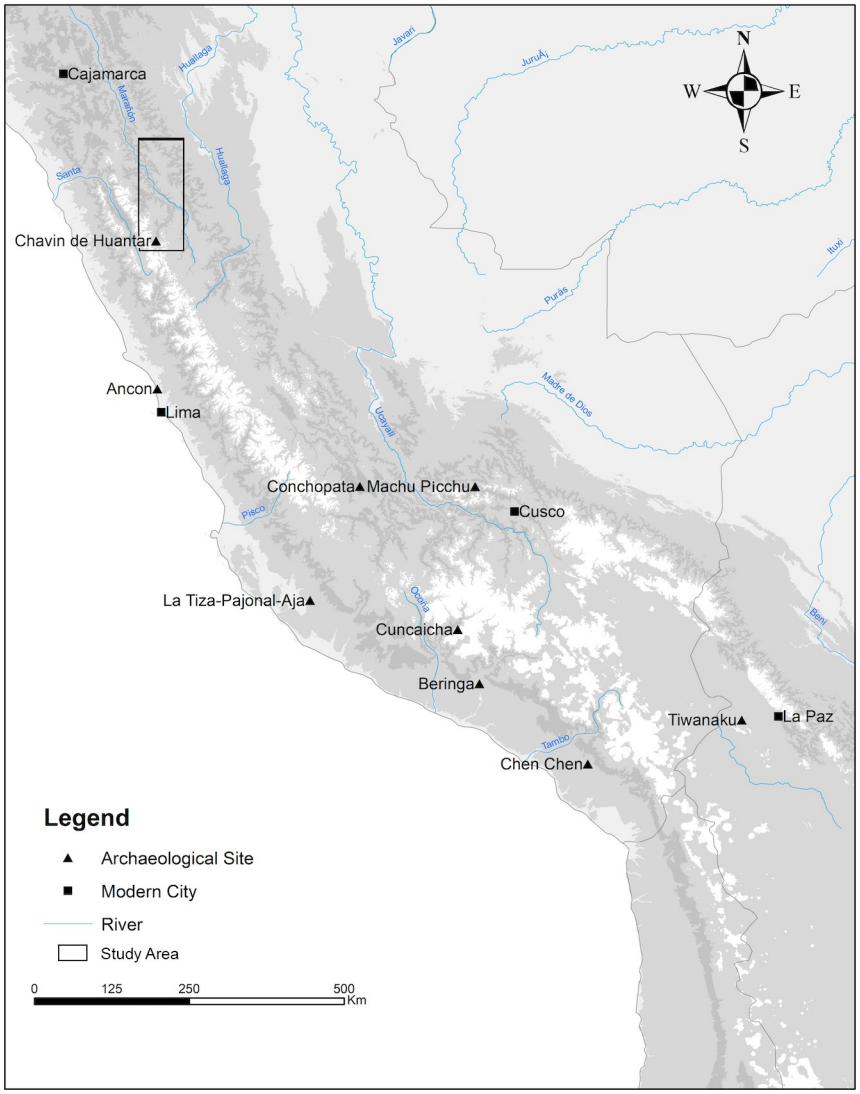

Fig 1. Map of Peru showing the Conchucos region, Department of Ancash (identified by black rectangle) as well as the locations of previous $^{87}Sr/^{86}Sr$ isotope studies throughout Peru. Map was produced in ArcGIS 10.4, with all subsequent layout and design preformed in Photoshop CC 14.2.

https://doi.org/10.1371/journal.pone.0248209.g001

rainfall, rivers, sea-spray, and wind-dust, also contribute to the bioavailable Sr in the food chain [15, 59, 71–74]. Modern anthropogenic Sr contaminations can be introduced through industrial fertilizers and even via dust from large scale construction sites [15, 59, 71, 75].

As organisms consume locally available food and water, these sources of Sr are mixed and incorporated into the organism's tissue [12, 42, 63]. In contrast to many commonly utilized light isotope systems, the isotopic composition of Sr does not change or fractionate during biological processes [63]. This is because the mass differences between the four Sr isotopes are relatively small [13, 62, 63, 76]. As a result, the $^{87}Sr/^{86}Sr$ values measured in flora and fauna vary mainly based on the age of the bedrock on which they sourced their nutrients. Very old bedrock with high Rb/Sr ratios will have the highest $^{87}Sr/^{86}Sr$ values today [58, 77]. Examples of geological deposits that have relatively high Rb/Sr ratios include clay-rich rocks such as shale, or igneous rocks that have high silica content, such as granite, with $^{87}Sr/^{86}Sr$ values up to 0.715

[13]. In contrast, geologically young rocks and sediments will have low Rb/Sr ratios and typically have $^{87}Sr/^{86}Sr$ less than 0.706 [e.g., 78]. To infer the biologically available $^{87}Sr/^{86}Sr$ values in an area, recent studies commonly use samples of uncontaminated environmental sources of local origin such as plants and small animals [59, 75, 79, 80], water [72, 81, 82] and soil [59] samples.

$^{87}Sr/^{86}Sr$ analysis in archaeology

While traditional archaeological approaches primarily rely on artifactual indications of population movement [16], the use of $^{87}Sr/^{86}Sr$ data obtained from human skeletal material allows researchers to directly examine individual mobility. Most studies employing $^{87}Sr/^{86}Sr$ analysis focus on the study of human skeletal remains from archaeological sites with the intention of identifying immigrants and to track residential mobility in the past [e.g., 3, 7–9, 83, 84]. $^{87}Sr/^{86}Sr$ studies have also been applied to address broader sociocultural questions relating to imperial strategies [17, 27, 28, 31, 32, 43, 51, 84, 85], colonization [31, 85–88], post-marital residential patterns [89–92], identity [37, 51, 93–95] and warfare [22, 36, 38, 96, 97].

As $^{87}Sr/^{86}Sr$ isotope analysis has been applied to address a wide range of archaeologically significant questions, methods for determining local $^{87}Sr/^{86}Sr$ ranges in the environment also continue to improve. Originally, researchers determined the local range of $^{87}Sr/^{86}Sr$ values as a two-standard deviation ($\pm 2\sigma$) range around the average $^{87}Sr/^{86}Sr$ value measured in all archaeological samples from a site, characterizing outliers as non-local individuals [15, 16]. This tends to produce a conservative estimate of non-locals in a population and may inadvertently underestimate the number of non-locals in a sample [15, 42, 98].

Given the potential challenges with defining local ranges based on mean calculations of the $^{87}Sr/^{86}Sr$ values of an ancient (and potentially highly mobile) human population, researchers now commonly sample local (both archaeological and modern) fauna and flora as proxies for locally bioavailable $^{87}Sr/^{86}Sr$ [5, 15–16, 20, 22, 32, 44, 98–101]. There are however, several considerations that should be made in sample selection [16]. In archaeological fauna, it is often unclear if animals were kept locally, remotely, or if they were subject to exchange. Depending on the source, modern domestic fauna may not reflect local $^{87}Sr/^{86}Sr$ values if they were fed imported, non-local foods, and/or if fodder was exposed to exogenic Sr though industrial fertilizers [15, 16, 59, 62]. Animals, or animal products, purchased from local markets where their geographic origin and/or the origin of their fodder may be unclear, can make associating the obtained $^{87}Sr/^{86}Sr$ data to a specific geological formation with the necessary certainty difficult [15, 31, 32].

In recent years there has also been an increased effort to create large-scale isoscapes, a spatially explicit prediction of isotopic variation across landscapes [42, 102–105]. An isoscape considers all published $^{87}Sr/^{86}Sr$ data for a given region and uses this dataset to extrapolate the extent of possible $^{87}Sr/^{86}Sr$ values across large geographic areas [71, 75, 106–111]. While these studies provide invaluable insight into the nature of past mobility on a population-wide pan-regional scale, they are dependent on the amount and quality of data used to generate the isoscape.

There are many approaches to conducting $^{87}Sr/^{86}Sr$ isotope research and each of these methods have advantages and limitations depending on the research questions and resolution of the data. In this study we present a detailed regional mapping project that emphasizes the collection of environmental samples of biologically available $^{87}Sr/^{86}Sr$, both within archaeological sites, as well as from the surrounding geological formations. This regional isoscape can then be applied to the study of human and animal mobility within the region.

Geology of the Peruvian Andes

The Central Andes are divided into the Cordillera Occidental to the west and the Cordillera Oriental to the east. The Cordillera Occidental is largely composed of late Cenozoic volcanic rocks such as andesites and Mesozoic formations. Age of the Cenozoic volcanic rock increases from the northern Andes to the southern Andes, and as a result the $^{87}Sr/^{86}Sr$ values are generally higher in the southern part of the Andes [78, 112]. $^{87}Sr/^{86}Sr$ values reported from late Cenozoic volcanic rocks in Ecuador exhibit $^{87}Sr/^{86}Sr$ values of 0.70431±0.00016 (1σ, n = 23) [112], while exposed bedrock samples from similar geologic formations in northern Chile exhibit mean $^{87}Sr/^{86}Sr$ values of 0.70646 ±0.00020 (1σ, n = 8) [78]. The Cordillera Oriental in the east is mainly comprised of Paleozoic geology. These formations generally have higher $^{87}Sr/^{86}Sr$ values than the western Cordillera; however, their $^{87}Sr/^{86}Sr$ values have not yet been measured in bedrock [61, 113]. In addition, on a broad pan-regional scale, $^{87}Sr/^{86}Sr$ values seemingly increase along a west to east gradient, with lower values along the Pacific coast (i.e., ~0.7038) and generally higher values moving inland to the east (~0.7239) [42].

Geographical and isotopic descriptions of the Andes in these broad terms do not adequately capture the geological complexity of this region, as depicted in Fig 2. It is because of this geological diversity that archaeologists are employing molecular tools such as $^{87}Sr/^{86}Sr$ analysis to address questions surrounding human life histories and population movements within the challenging landscape of the Andes [e.g., 17, 20–22, 50, 100].

Material and study region

The study area consists of a broad swath of the eastern highlands of north-central Peru known as the Conchucos region. Conchucos is an intermontane valley system situated on the southeastern side of the Cordillera Blanca and is characterized by several rivers that drain into the Marañón River, one of the major tributaries of the Amazon. Our study focuses on sample collection over an area of 2,640 km^2 that includes the Huaritambo, Mosna/Puccha, and Marañón rivers. This region is archaeologically rich [e.g., 70], with archaeological sites dating from ca. 1100 BCE until the 16th century [e.g., 114–126].

As illustrated in Fig 2, the Conchucos region is geologically diverse. The predominant geology comprises folded Mesozoic sedimentary rock formations, including sandstones, dark shales, and carbonates (limestone, marls, and dolomites), as well as metamorphic rocks like quartzite and slate [127–129]. The entire region is shaped by these folded and uplifted layers of bedrock that causes the repetition of specific geologic units over a broad area. This is important to consider when defining the categories of local and non-local populations in the archaeological record based on $^{87}Sr/^{86}Sr$ values, as similar geological units can be found throughout the landscape. Towards the north and east the study area is bordered by the geological Marañón Group. Dating to the Proterozoic, Marañón Group rocks are much older than the other formations and consist of meta-sedimentary schists, gneiss, and red sandstone [130].

To assess bioavailable $^{87}Sr/^{86}Sr$ values, we collected empty shells of modern terrestrial snails (Bulimulidae), as well as wild perennial grasses abundant in the Peruvian highlands (i.e. *Stipa ichu*) (Table 1; Fig 2). Snail shells are plentiful on the landscape and make it unnecessary to obtain live animals. Snails are additionally limited in the extent of their movement throughout their lifetime and can therefore be considered representative of local variability in bioavailable $^{87}Sr/^{86}Sr$ [83, 131, 132]. Sr is deposited in the snail shell, where it substitutes for its main component Ca [133]. Plant $^{87}Sr/^{86}Sr$ values reflect the $^{87}Sr/^{86}Sr$ values in the immediate local soil, as well as $^{87}Sr/^{86}Sr$ admixture introduced by rainwater and atmospheric dust [131].

During field sampling, major geological formations in the region were identified using a geological map [129]. We obtained 100 modern environmental reference samples from 14

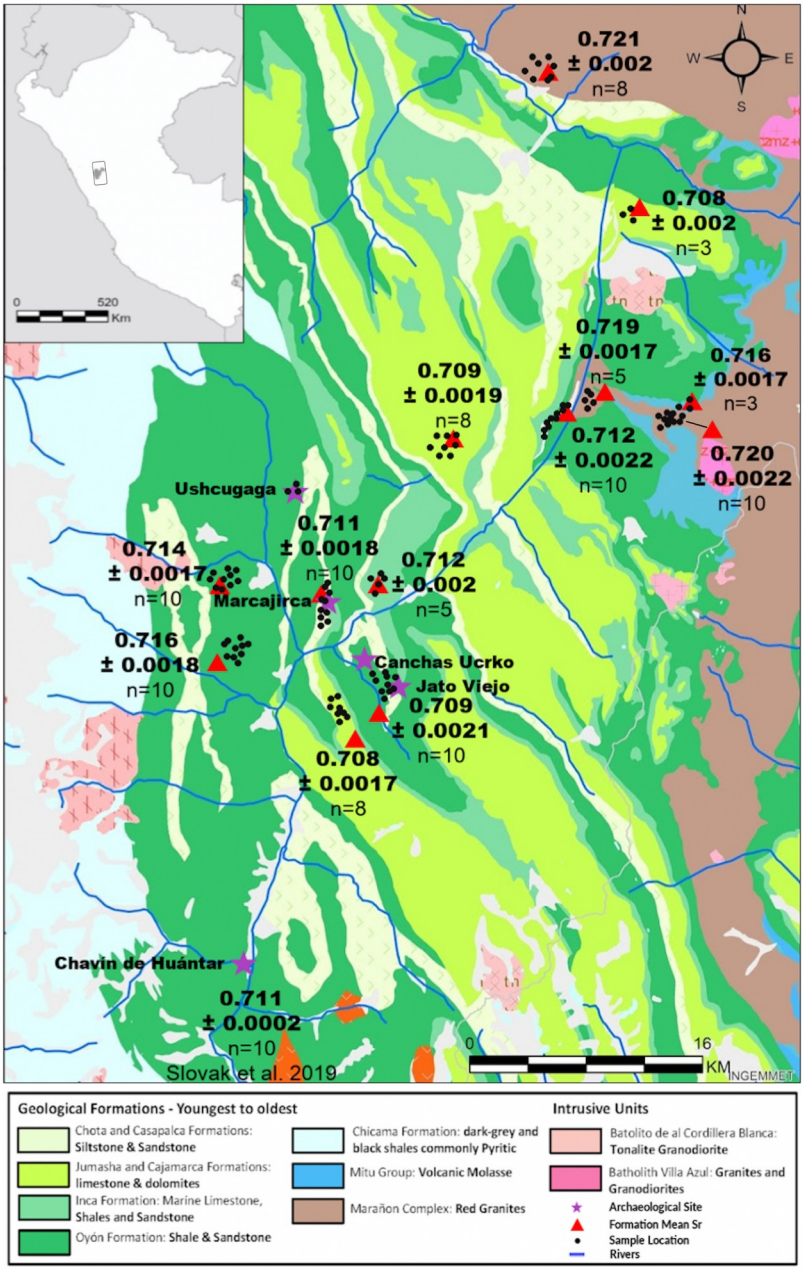

Fig 2. $^{87}Sr/^{86}Sr$ isoscape of the Conchucos region in the north-central Peruvian highlands. Environmental reference samples include grass (*Stipa ichu)* and snail shells (Bulimulidae). Mean $^{87}Sr/^{86}Sr$ values were calculated for each geological formation and are presented along with mean standard error. Individual sampling locations are identified by black dots. Map was produced in ArcGIS 10.4, with all subsequent layout and design preformed in Photoshop CC 14.2.

https://doi.org/10.1371/journal.pone.0248209.g002

sampling sites in six geological units covering a 3,840 km^2 area of the Conchucos region. In each geological unit, we selected sampling locations where anthropogenic contamination through fertilizers or other pollutants were unlikely, as there were no signs of use through agriculture and there was considerable distance to roads and/or towns. At each location we collected snail shells from the surface alongside several samples of *Stipa ichu* (3–10 plants/unit).

Table 1. Results of $^{87}Sr/^{86}Sr$ environmental sampling from six geological formations within the Conchucos region of Peru; sorted by sampling location.

Lab Code	Sample	Geological Formation	Geological Age	Latitude	Longitude	$^{87}Sr/^{86}Sr$	StdErr (%)
HAGS 1	Bulimulidae	Casapalca, Chota, Huaylas	Cenozoic to Mesozoic	S 09˚22'23.8"	W077˚07'49.5"	0.7113	0.0015
HAGS 2	Bulimulidae	Casapalca, Chota, Huaylas	Cenozoic to Mesozoic	S 09˚22'11.91"	W077˚07'49.39"	0.7111	0.00147
HAGS 3	Bulimulidae	Casapalca, Chota, Huaylas	Cenozoic to Mesozoic	S 09˚22'14.09"	W077˚07'49.47"	0.7104	0.00232
HAGS 4	Bulimulidae	Casapalca, Chota, Huaylas	Cenozoic to Mesozoic	S 09˚22'15.74"	W077˚07'49.56	0.71140	0.0022
HAGS 5	Bulimulidae	Casapalca, Chota, Huaylas	Cenozoic to Mesozoic	S 09˚22'17.40"	W077˚07'49.71"	0.7114	0.00159
HAGS 6	*Stipa ichu*	Casapalca, Chota, Huaylas	Cenozoic to Mesozoic	S 09˚22'27.7"	W077˚07'50.3"	0.7108	0.00247
HAGS 7	*Stipa ichu*	Casapalca, Chota, Huaylas	Cenozoic to Mesozoic	S 09˚22.24.9"	W077˚07'49.2"	0.7107	0.0018
HAGS 8	*Stipa ichu*	Casapalca, Chota, Huaylas	Cenozoic to Mesozoic	S 09˚22'18.33"	W077˚07'49.76"	0.7109	0.00145
HAGS 9	*Stipa ichu*	Casapalca, Chota, Huaylas	Cenozoic to Mesozoic	S 09˚22'19.66"	W077˚07'49.11"	0.7113	0.00185
HAGS 10	*Stipa ichu*	Casapalca, Chota, Huaylas	Cenozoic to Mesozoic	S 09˚22'21.26"	W077˚07'49.93"	0.7109	0.00154
Mean						**0.71102**	**0.0018**
HAGS 11	Bulimulidae	Casapalca, Chota, Huaylas	Cenozoic to Mesozoic	S 09˚13'56.7"	W076˚58'18.7"	0.7113	0.00225
HAGS 12	Bulimulidae	Casapalca, Chota, Huaylas	Cenozoic to Mesozoic	S 09˚13'57.3"	W076˚58'18.8"	0.7108	0.00243
HAGS 13	Bulimulidae	Casapalca, Chota, Huaylas	Cenozoic to Mesozoic	S 09˚13'48.0"	W076˚58'14.2"	0.7139	0.00281
HAGS 14	Bulimulidae	Casapalca, Chota, Huaylas	Cenozoic to Mesozoic	S 09˚13'55.5"	W076˚58'19.3"	0.7102	0.00285
HAGS 15	Bulimulidae	Casapalca, Chota, Huaylas	Cenozoic to Mesozoic	S 09˚13'57.3"	W076˚58'17.2"	0.7123	0.0029
HAGS 16	*Stipa ichu*	Casapalca, Chota, Huaylas	Cenozoic to Mesozoic	S 09˚13'47.2"	W076˚58'13.8"	0.7141	0.00166
HAGS 17	*Stipa ichu*	Casapalca, Chota, Huaylas	Cenozoic to Mesozoic	S 09˚13'55.70"	W076˚58'17.73"	0.7107	0.00145
HAGS 18	*Stipa ichu*	Casapalca, Chota, Huaylas	Cenozoic to Mesozoic	S 09˚13'50.43"	W076˚58'14.17"	0.7138	0.00206
HAGS 19	*Stipa ichu*	Casapalca, Chota, Huaylas	Cenozoic to Mesozoic	S 09˚13'47.2"	W076˚58'13.8"	0.7113	0.00162
HAGS 20	*Stipa ichu*	Casapalca, Chota, Huaylas	Cenozoic to Mesozoic	S 09˚14'25.2"	W076˚54'16.3"	0.7109	0.00207
Mean						**0.7119**	**0.00222**
HAGS 21	Bulimulidae	Jumasha, Celendin, and Cajamarca	Mesozoic	S 09˚23'34.7"	W077˚08'09.9"	0.7083	0.00182
HAGS 22	Bulimulidae	Jumasha, Celendin, and Cajamarca	Mesozoic	S 09˚23'30.3"	W077˚08'06.6"	0.7081	0.00143
HAGS 23	Bulimulidae	Jumasha, Celendin, and Cajamarca	Mesozoic	S 09˚23'35.03"	W077˚08'08.62"	0.7078	0.00167
HAGS 24	Bulimulidae	Jumasha, Celendin, and Cajamarca	Mesozoic	S 09˚23'35.77"	W077˚08'10.13"	0.7089	0.00175
HAGS 25	Bulimulidae	Jumasha, Celendin, and Cajamarca	Mesozoic	S 09˚23'34.77"	W077˚08'11.45"	0.7084	0.00146
HAGS 26	*Stipa ichu*	Jumasha, Celendin, and Cajamarca	Mesozoic	S 09˚23'30.3"	W077˚08'06.6"	0.7078	0.00232
HAGS 27	*Stipa ichu*	Jumasha, Celendin, and Cajamarca	Mesozoic	S 09˚23'32.97"	W077˚08'11.14"	0.7081	0.00171
HAGS 28	*Stipa ichu*	Jumasha, Celendin, and Cajamarca	Mesozoic	S 09˚23'31.99"	W077˚08'06.09"	0.7087	0.00166
Mean						**0.7083**	**0.0017**
HAGS 29	Bulimulidae	Jumasha, Celendin, and Cajamarca	Mesozoic	S 09˚15'7.98"	W077˚03'22.52"	0.7083	0.00175
HAGS 30	Bulimulidae	Jumasha, Celendin, and Cajamarca	Mesozoic	S 09˚15'3.73"	W077˚02'54.14"	0.7092	0.00156
HAGS 31	Bulimulidae	Jumasha, Celendin, and Cajamarca	Mesozoic	S 09˚15'27.39""	W077˚03' 37.08"	0.7079	0.00167
HAGS 32	Bulimulidae	Jumasha, Celendin, and Cajamarca	Mesozoic	S 09˚15'39.97"	W077˚03'53.99"	0.7087	0.0019
HAGS 33	Bulimulidae	Jumasha, Celendin, and Cajamarca	Mesozoic	S 09˚16'16.30"	W077˚03'14.55"	0.7094	0.00146
HAGS 34	*Stipa ichu*	Jumasha, Celendin, and Cajamarca	Mesozoic	S 09˚16'5.40"	W077˚02'52.40"	0.7093	0.00232
HAGS 35	*Stipa ichu*	Jumasha, Celendin, and Cajamarca	Mesozoic	S 09˚14' 33.43	W077˚03'22.03"	0.7084	0.00275
HAGS 36	*Stipa ichu*	Jumasha, Celendin, and Cajamarca	Mesozoic	S 09˚14'38.64"	W077˚04'30.78"	0.7087	0.00163
Mean						**0.7087**	**0.0019**
HAGS 37	Bulimulidae	Jumasha, Celendin, and Cajamarca	Mesozoic	S 09˚6'12.97"	W076˚56'54.33"	0.7082	0.0024
HAGS 38	*Stipa ichu*	Jumasha, Celendin, and Cajamarca	Mesozoic	S 09˚6'24.25"	W076˚56'31.54"	0.7081	0.002
HAGS 39	*Stipa ichu*	Jumasha, Celendin, and Cajamarca	Mesozoic	S 09˚6'14.00"	W076˚56'35.72"	0.7087	0.0018
Mean						**0.7083**	**0.002**
HAGS 40	Bulimulidae	Oyón, Huaalhuani and Murco	Mesozoic	S 09˚24'24.3"	W077˚06'09.7"	0.7092	0.00154
HAGS 41	Bulimulidae	Oyón, Huaalhuani and Murco	Mesozoic	S 09˚24'23.06"	W077˚06'09.62"	0.7091	0.00208
HAGS 42	Bulimulidae	Oyón, Huaalhuani and Murco	Mesozoic	S 09˚24'23.89"	W077˚06'09.40"	0.7087	0.00181

(*Continued*)

Table 1. (Continued)

Lab Code	Sample	Geological Formation	Geological Age	Latitude	Longitude	$^{87}Sr/^{86}Sr$	StdErr (%)
HAGS 43	Bulimulidae	Oyón, Huaalhuani and Murco	Mesozoic	S 09˚24'22.00"	W077˚06'09.94"	0.7092	0.00193
HAGS 44	Bulimulidae	Oyón, Huaalhuani and Murco	Mesozoic	S 09˚24'24.3"	W077˚06'09.72"	0.7108	0.00174
HAGS 45	*Stipa ichu*	Oyón, Huaalhuani and Murco	Mesozoic	S 09˚24'22.12"	W077˚06'10.46"	0.7092	0.00283
HAGS 46	*Stipa ichu*	Oyón, Huaalhuani and Murco	Mesozoic	S 09˚24'23.51"	W077˚06'10.07"	0.7089	0.00293
HAGS 47	*Stipa ichu*	Oyón, Huaalhuani and Murco	Mesozoic	S 09˚24'24.88"	W077˚06'09.53"	0.7084	0.00167
HAGS 48	*Stipa ichu*	Oyón, Huaalhuani and Murco	Mesozoic	S 09˚24'24.88"	W077˚06'09.10"	0.7082	0.00256
HAGS 49	*Stipa ichu*	Oyón, Huaalhuani and Murco	Mesozoic	S 09˚24'24.34"	W077˚06'09.25"	0.7089	0.00184
Mean						**0.7091**	**0.0021**
HAGS 50	Bulimulidae	Oyón, Huaalhuani and Murco	Mesozoic	S 09˚23'21.9"	W077˚10'31.9"	0.7158	0.0016
HAGS 51	Bulimulidae	Oyón, Huaalhuani and Murco	Mesozoic	S 09˚23'23.5"	W077˚10'34.0"	0.7179	0.00187
HAGS 52	Bulimulidae	Oyón, Huaalhuani and Murco	Mesozoic	S 09˚23'22.8"	W077˚10'34.6"	0.7172	0.00131
HAGS 53	Bulimulidae	Oyón, Huaalhuani and Murco	Mesozoic	S 09˚23'21.23"	W077˚10'33.32"	0.7164	0.00204
HAGS 54	Bulimulidae	Oyón, Huaalhuani and Murco	Mesozoic	S 09˚23'21.68"	W077˚10'35.90"	0.7159	0.00184
HAGS 55	*Stipa ichu*	Oyón, Huaalhuani and Murco	Mesozoic	S 09˚23'21.2"	W077˚10'31.7"	0.7164	0.00251
HAGS 56	*Stipa ichu*	Oyón, Huaalhuani and Murco	Mesozoic	S 09˚23'20.2"	W077˚10'32.9"	0.7151	0.00158
HAGS 57	*Stipa ichu*	Oyón, Huaalhuani and Murco	Mesozoic	S 09˚23.329"	W077˚10.33.7"	0.7157	0.00224
HAGS 58	*Stipa ichu*	Oyón, Huaalhuani and Murco	Mesozoic	S 09˚23'22.2"	W077˚10'32.8"	0.7159	0.00175
HAGS 59	*Stipa ichu*	Oyón, Huaalhuani and Murco	Mesozoic	S 09˚23'22.2"	W077˚10'33.2"	0.7161	0.00145
Mean						**0.7162**	**0.0018**
HAGS 60	Bulimulidae	Oyón, Huaalhuani and Murco	Mesozoic	S 09˚2106.9"	W077˚11'23.0"	0.7142	0.0016
HAGS 61	Bulimulidae	Oyón, Huaalhuani and Murco	Mesozoic	S 09˚21'08.2"	W077˚11'20.2"	0.7133	0.00242
HAGS 62	Bulimulidae	Oyón, Huaalhuani and Murco	Mesozoic	S 09˚21'05.4"	W077˚11'15.9"	0.7139	0.00163
HAGS 63	Bulimulidae	Oyón, Huaalhuani and Murco	Mesozoic	S 09˚21'05.8"	W077˚11'14.7"	0.7141	0.0007
HAGS 64	Bulimulidae	Oyón, Huaalhuani and Murco	Mesozoic	S 09˚21'07.27"	W077˚11'17.47"	0.7128	0.00236
HAGS 65	*Stipa ichu*	Oyón, Huaalhuani and Murco	Mesozoic	S 09˚21'05.2"	W077˚11'18.5"	0.7134	0.00197
HAGS 66	*Stipa ichu*	Oyón, Huaalhuani and Murco	Mesozoic	S 09˚21'07.1"	W077˚11'12.6"	0.7142	0.00307
HAGS 67	*Stipa ichu*	Oyón, Huaalhuani and Murco	Mesozoic	S 09˚21'07.37"	W077˚11'15.74"	0.7138	0.00175
HAGS 68	*Stipa ichu*	Oyón, Huaalhuani and Murco	Mesozoic	S 09˚21'03.28"	W077˚11'15.24"	0.7141	0.0006
HAGS 69	*Stipa ichu*	Oyón, Huaalhuani and Murco	Mesozoic	S 09˚21'03.10"	W077˚11'20.21"	0.7134	0.00247
Mean						**0.7137**	**0.0019**
HAGS 70	Bulimulidae	Inca, Pariahuanca, chúlec Pariatambo	Mesozoic	S 09˚21'2.44 "	W077˚5'35.66"	0.7123	0.00134
HAGS 71	Bulimulidae	Inca, Pariahuanca, chúlec Pariatambo	Mesozoic	S 09˚21'39.05"	W077˚5'31.39"	0.7121	0.00252
HAGS 72	*Stipa ichu*	Inca, Pariahuanca, chúlec Pariatambo	Mesozoic	S 09˚21'23.49"	W077˚5'14.96"	0.7129	0.00162
HAGS 73	*Stipa ichu*	Inca, Pariahuanca, chúlec Pariatambo	Mesozoic	S 09˚21'7.91"	W077˚5'59.54"	0.7121	0.00153
HAGS 74	*stipa ichu*	Inca, Pariahuanca, chúlec Pariatambo	Mesozoic	S 09˚21'42.17"	W077˚5'40.25"	0.7126	0.00234
Mean						**0.7124**	**0.002**
HAGS 75	*Stipa ichu*	Pucará Group	Paleozoic	S 09˚14'10.39 "	W076˚54'43.81"	0.7163	0.00231
HAGS 76	*Stipa ichu*	Pucará Group	Paleozoic	S 09˚14'15.54 "	W076˚55'1.53"	0.7154	0.00123
HAGS 77	*Stipa ichu*	Pucará Group	Paleozoic	S 09˚14'5.98"	W076˚55'15.38"	0.7158	0.00166
Mean						**0.7158**	**0.0017**
HAGS 78	Bulimulidae	Marañón Group	Neoproterozoic	S 09˚14'25.92"	W076˚54'17.51"	0.7198	0.00179
HAGS 79	Bulimulidae	Marañón Group	Neoproterozoic	S 09˚14'28.26"	W076˚54'18.67"	0.7207	0.00212
HAGS 80	Bulimulidae	Marañón Group	Neoproterozoic	S 09˚14'29.93"	W076˚54'16.72"	0.7212	0.00146
HAGS 81	Bulimulidae	Marañón Group	Neoproterozoic	S 09˚14'28.10"	W076˚54'14.52"	0.7214	0.00237
HAGS 82	Bulimulidae	Marañón Group	Neoproterozoic	S 09˚14'30.79"	W076˚54'12.78"	0.7202	0.00253
HAGS 83	*Stipa ichu*	Marañón Group	Neoproterozoic	S 09˚14'33.0"	W076˚54'09.6"	0.7159	0.00223
HAGS 84	*Stipa ichu*	Marañón Group	Neoproterozoic	S 09˚14'29.7"	W076˚54'14.9"	0.7197	0.00358

(*Continued*)

Table 1. (Continued)

Lab Code	Sample	Geological Formation	Geological Age	Latitude	Longitude	$^{87}Sr/^{86}Sr$	StdErr (%)
HAGS 85	*Stipa ichu*	Marañón Group	Neoproterozoic	S 09˚14'29.4"	W076˚54'18.2"	0.7215	0.00253
HAGS 86	*Stipa ichu*	Marañón Group	Neoproterozoic	S 09˚14'29.1"	W076˚54'19.6"	0.7187	0.00243
HAGS 87	*Stipa ichu*	Marañón Group	Neoproterozoic	S 09˚14'32.20"	W076˚54'10.85"	0.7208	0.00126
Mean						**0.7200**	**0.0022**
HAGS 88	Bulimulidae	Marañón Group	Neoproterozoic	S 09˚14' 8.26"	W076˚57'45.70"	0.7179	0.00172
HAGS 89	Bulimulidae	Marañón Group	Neoproterozoic	S 09˚13'56.75"	W076˚57'43.34"	0.7187	0.00125
HAGS 90	*Stipa ichu*	Marañón Group	Neoproterozoic	S 09˚14' 5.09"	W076˚57'59.32"	0.7192	0.00223
HAGS 91	*Stipa ichu*	Marañón Group	Neoproterozoic	S 09˚13'54.91 "	W076˚58'3.08"	0.7194	0.00164
HAGS 92	*Stipa ichu*	Marañón Group	Neoproterozoic	S 09˚14' 12.27"	W076˚58'1.29"	0.7184	0.00143
Mean						**0.7187**	**0.0017**
HAGS 93	Bulimulidae	Marañón Group	Neoproterozoic	S 09˚0'6.11"	W077˚1'2.29"	0.7208	0.00223
HAGS 94	Bulimulidae	Marañón Group	Neoproterozoic	S 09˚0'5.07 "	W077˚1'32.08"	0.7206	0.00235
HAGS 95	Bulimulidae	Marañón Group	Neoproterozoic	S 09˚0'46.10 "	W077˚0'59.93"	0.7203	0.00124
HAGS 96	Bulimulidae	Marañón Group	Neoproterozoic	S 09˚0'22.11"	W077˚0'45.79."	0.7212	0.00246
HAGS 97	Bulimulidae	Marañón Group	Neoproterozoic	S 09˚0'13.72"	W077˚0'29.21"	0.7205	0.00129
HAGS 98	*Stipa ichu*	Marañón Group	Neoproterozoic	S 09˚0'3.83"	W077˚1'22.60"	0.7206	0.00238
HAGS 99	*Stipa ichu*	Marañón Group	Neoproterozoic	S 09˚0'37.89 "	W077˚0'54.38"	0.7196	0.00229
HAGS 100	*Stipa ichu*	Marañón Group	Neoproterozoic	S 09˚0'37.57 "	W077˚0'54.78"	0.7198	0.00231
Mean						**0.7205**	**0.020**

https://doi.org/10.1371/journal.pone.0248209.t001

Each sample location was recorded via a hand-held GPS. Import permits for all plants and snail shells were granted by the United States Department of Agriculture, Animal and Plant Health Inspection Service (Permit Number: PCIP-18-00364). No export permits were required for the sample material used in this study.

Methods

Sample preparation was conducted in the Primate Ecology and Molecular Anthropology laboratory (PEMA) at the University of California at Santa Cruz (UCSC). Snail shells were repeatedly rinsed with ddH_2O in an ultrasonic bath to remove any attached sediment. Snail shells were then broken into smaller fragments, placed in individual beakers with ultrapure acetone, rinsed in an ultrasonic bath for another 15 minutes to remove any potential contaminants on the shell surface and were then set to dry. Plant samples (2g of well- dried plant material) and snail shells (~300mg) were then ashed at 800˚C for 12 hours in a muffle furnace. The remaining ash (n = 100 samples) was transferred to the UCSC W.M. Keck Isotope Laboratory clean room, where 20mg of ash from each sample was weighed into clean Teflon beakers and digested for 2 hours in 2ml of 65% HNO_3 on a hot plate set to 120˚C. Due to the cell structure of plant material, complete digestion of plant ash was difficult, thus these samples were subjected to a microwave digestion in an Anton Paar Multiwave GO Microwave Digestion System. Ashed plant material was combined with 8ml of 65% HNO_3 and 1ml of 6M HCL in a pressure vessel for approximately 30 mins. The dissolved samples of snail shell and microwave digested plants were then placed in open Teflon beakers on a hot plate at 120˚C for at least 8 hours to evaporate. Following this, samples were resolved in 1ml of 3M HNO_3. Each sample was carefully transferred into pre-conditioned chromatography columns containing clean Sr-spec™ resin. Samples were reloaded through the resin three times to maximize the amount of Sr attaching to the resin. After 3 washes with 3M HNO_3, the strontium was eluted from the resin with ultrapure ddH_2O into clean Teflon beakers and dried down on a hotplate. The

remaining sample, again re-dissolved in 5% HNO_3 was dip checked on the Thermo Finnigan Neptune™ MC-ICP-MS instrument to check the concentration of Sr in each sample. Any sample that had a $v^{88}SR$ value above 40ppm was diluted down to ~40ppm ($v^{88}SR$). Samples were then measured parallel to the SRM 987 standard, procedural blanks (one/every batch of 9 samples), as well as one clean acid blank after every 5 samples, in a Thermo Finnigan Neptune™ MC-ICP-MS.

Results

We measured $^{87}Sr/^{86}Sr$ in 100 environmental samples (50 snail shells and 50 plant samples). Repeated $^{87}Sr/^{86}Sr$ measurement of the SRM 987 standard resulted in an average value of 0.7093 ±0.00013. The procedural blanks, one for each batch of nine samples, showed negligible amounts of Sr, indicating no sample cross contamination. $^{87}Sr/^{86}Sr$ measured in 50 plant samples range from 0.7071 to 0.7215. $^{87}Sr/^{86}Sr$ measured in 50 snail shell samples range from 0.7078 to 0.7214 (Table 1; Fig 2). Mean $^{87}Sr/^{86}Sr$ values for each sampling location as well as more detailed information on each geological unit are presented in Table 1.

Discussion

The use of $^{87}Sr/^{86}Sr$ isoscapes: What does it mean to be a "local"?

Within relatively short distances between sampling locations, we documented considerable differences in mean $^{87}Sr/^{86}Sr$ values per geological unit that range from as low as 0.7078 to 0.7212 within 10km distance (Fig 2). This suggests that in these geological settings, ancient farming, animal husbandry and hunting would likely result in the utilization of several larger geological units with distinct geological ages and $^{87}Sr/^{86}Sr$ values. We can extend this statement to other locations within the Conchucos region. This finding has important implications for archaeological research interested in understanding past human mobility not only in this specific region, but throughout the Andes.

The analysis of $^{87}Sr/^{86}Sr$ values in human skeletal remains is a powerful tool to reconstruct past human mobility. However, the interpretation of $^{87}Sr/^{86}Sr$ data are not always straightforward. Individuals with $^{87}Sr/^{86}Sr$ values outside the estimated local $^{87}Sr/^{86}Sr$ range of a given site are commonly described as having consumed non-local sources of Sr, either by they themselves being non-locals or by consuming non-local foods (i.e. through trade or consuming foods farmed in a geologically distinct region) [1, 7, 8, 30–36, 43, 44]. Whereas those with $^{87}Sr/^{86}Sr$ values matching those of the immediate vicinity of the site are considered to have consumed local sources of Sr and were therefore potential residents of that site [1, 7, 8, 30–36, 59]. To address questions surrounding residential mobility requires not only $^{87}Sr/^{86}Sr$ data but also nuanced interpretations of archaeological context and potentially the use of light isotopes (i.e. Carbon and Nitrogen) to estimate diet. Our data illustrates that even locally residing individuals can potentially have a range of sources of $^{87}Sr/^{86}Sr$ values within a discrete area, depending on where they farmed their plants and produced their animal food. If the $^{87}Sr/^{86}Sr$ values measured in enamel are represented in the region surrounding an archaeological site, they may be considered potentially local.

In the highland Andes, archaeological sites are frequently located along ecological boundaries, allowing their inhabitants to exploit multiple ecological zones that cross different geological formations [48, 57, 134–146]. This may have been achieved through connections with populations living in different ecological zones that were linked to each other by exchange and/or kinship relationships, [57, 134, 147–149], or mobile groups who camped at different zones to access resources seasonally [134, 136, 138, 150].

Because the $^{87}Sr/^{86}Sr$ value of a given tissue (i.e., bone or tooth enamel) is an average of all the bioavailable $^{87}Sr/^{86}Sr$ ingested over the duration of that tissues' formation [59, 109, 151], the extent of landscape-use related mobility should be considered, especially within regions that are as ecologically and geologically complex as the Andes. If enamel of late forming teeth is used and individuals are frequently consuming dietary items of different geological origin, their $^{87}Sr/^{86}Sr$ values will be a mix of the $^{87}Sr/^{86}Sr$ values of these consumed food sources. For example, if an adult individual's $^{87}Sr/^{86}Sr$ value does not fit within the bioavailable $^{87}Sr/^{86}Sr$ range of a given site that does not necessarily mean this person should be considered non-local. Rather, this may indicate a higher degree of local mobility within the framework of farming and hunting. On the other hand, even though a region is geologically diverse, if individuals were not utilizing the entire landscape human $^{87}Sr/^{86}Sr$ values may not be variable. It is for this reason that establishing baseline environmental $^{87}Sr/^{86}Sr$ isotope data from within archaeological sites as well as from the surrounding landscape is crucial to a more thorough examination of past human mobility.

For example, in a recent study Slovak and colleagues [44] report the first $^{87}Sr/^{86}Sr$ signatures from five human Mariash-Recuay individuals (ca. AD 1–700) buried at the Peruvian highland ceremonial center of Chavín de Huántar (3,180 masl) located in our study region (Fig 2). To establish a local bioavailable $^{87}Sr/^{86}Sr$ range, several soil, animal and plant samples collected from within and around the ceremonial center (~2ha) were analyzed [44]. Based on these reference samples, three Chavín human individuals were classified to be of local origin (CdH_38, 39, 40 $^{87}Sr/^{86}Sr$ = 0.7111–0.7113), whereas two others with $^{87}Sr/^{86}Sr$ values outside the estimated local range (CdH_36 $^{87}Sr/^{86}Sr$ = 0.708; CdH_37 $^{87}Sr/^{86}Sr$ = 0.706) were considered to be of non-local origin. Slovak and colleagues [44] report potential regions of origin that range from the central coast to the Atacama Desert.

Based on our data, we propose that while it is possible that individual CdH_36 ($^{87}Sr/^{86}Sr$ value of 0.708) may have migrated to Chavín de Huántar from much further distances, this individual may have had a life history background in the Conchucos region and moved to Chavín de Huántar after early childhood (as premolars and second molars were used in this study). $^{87}Sr/^{86}Sr$ values similar to this individual can be found in the vicinity of Chavín de Huántar such as within the Jumasha and Cajamarca formations, only 10 km away, where we report $^{87}Sr/^{86}Sr$ values of 0.708 ±0.0017 (Fig 2).

Comparing a pan-Andean isoscape to our regionally specific $^{87}Sr/^{86}Sr$ study

In a recent publication, Scaffidi and Knudson [42] present a pan-Andean isoscape that combines all published $^{87}Sr/^{86}Sr$ data prior to 2019 from Peru, and applies geostatistical modeling to generate a predictive model for $^{87}Sr/^{86}Sr$ values found within the Andes. As discussed by Scaffidi and Knudson [42], this extensive dataset has the potential to be particularly valuable in regions where baseline environmental sampling is logistically or contextually problematic and/or those regions of Peru lacking $^{87}Sr/^{86}Sr$ reference data. Until recently, the majority of $^{87}Sr/^{86}Sr$ studies within Peru have taken place either along the Pacific coast or in the southern Andes particularly along the western slopes, with very few studies in the eastern highlands (Fig 2; [e.g., 17–52]). In this isoscape, regions with little to no $^{87}Sr/^{86}Sr$ reference data are presented as geologically and isotopically uniform. This affects the projection of $^{87}Sr/^{86}Sr$ values for the Conchucos region, for which we present highly variable environmental data.

Scaffidi and Knudson [42] show a general pattern of a west to east gradient of lesser to greater radiogenic values, with lower $^{87}Sr/^{86}Sr$ values along the coast (i.e., 0.7038–0.70550 coastal) and generally higher values moving towards the east (0.7177–0.7239). While on a

macro-scale and over large distances this distinction is observed, our study suggests that there is also considerable geological variation in the Conchucos region, a small area totaling only 0.4% of Peru. Within the Conchucos region, we document more extensive isotopic variation than initially estimated, including relatively low and relatively radiogenic $^{87}Sr/^{86}Sr$ values (0.7078–0.7212).

The geology of the Andes is comprised of closely stacked geological formations that run in parallel from north to south. Our study demonstrates that because each of these geological formations is of distinct geologic age, there are differing $^{87}Sr/^{86}Sr$ values represented within close proximity. In contrast to the pan-Andean isoscape created by Scaffidi and Knudson [42], within our localized study region there does not appear to be a west-east trend in $^{87}Sr/^{86}Sr$ values. In this region the lowest $^{87}Sr/^{86}Sr$ value (0.7078) is found in Jumasha and Cajamarca formations that run in between geological formations with higher $^{87}Sr/^{86}Sr$ values (0.7133–0.7178 to the west; 0.7196–0.7208 to the east).

The entire range of documented $^{87}Sr/^{86}Sr$ values in all archaeological Andean samples measured to date is 0.7038–0.7234 [42], which is just as broad as reported globally [59]. Interestingly, within the Conchucos isoscape we report a similar range of environmental $^{87}Sr/^{86}Sr$ values (0.7078–0.7212). Based on our data, we can predict that this environmental degree of $^{87}Sr/^{86}Sr$ variation will be present throughout the Andes. The results of our regional isoscape have the potential to fine tune the resolution of this pan-Andean isoscape.

Conclusion

This study contributes to the achievements of previous $^{87}Sr/^{86}Sr$ isotope studies within Peru by providing a novel and detailed $^{87}Sr/^{86}Sr$ isoscape for the previously understudied Conchucos region. We also address the challenge with the application of $^{87}Sr/^{86}Sr$ data in making determinations about past human mobility. Our data illustrates the need to consider a larger scope of possibilities to explain why an individual may have an $^{87}Sr/^{86}Sr$ value outside of the expected local range.

Acknowledgments

We thank Terry Blackburn, Brian Dryer and the W.M. Keck Laboratory Staff for their continued support with isotope analysis. For their contributions to sample collection in the field, we also thank Rachel Johnson and Alana Garvey. Finally, we gratefully acknowledge Jelmer Eerkens and Judith Habicht-Mauche for their invaluable input and support throughout this project. Import permits for all plants and snail shells were granted by the United States Department of Agriculture, Animal and Plant Health Inspection Service (PCIP-18-00364).

Author Contributions

Conceptualization: Eden Washburn, Jason Nesbitt, Bebel Ibarra, Lars Fehren-Schmitz.

Data curation: Eden Washburn.

Formal analysis: Eden Washburn, Lars Fehren-Schmitz, Vicky M. Oelze.

Funding acquisition: Eden Washburn, Lars Fehren-Schmitz.

Investigation: Eden Washburn, Bebel Ibarra, Lars Fehren-Schmitz.

Methodology: Eden Washburn, Jason Nesbitt, Lars Fehren-Schmitz, Vicky M. Oelze.

Resources: Eden Washburn, Jason Nesbitt, Bebel Ibarra.

Supervision: Jason Nesbitt, Lars Fehren-Schmitz, Vicky M. Oelze.

Writing – original draft: Eden Washburn, Jason Nesbitt, Bebel Ibarra, Lars Fehren-Schmitz, Vicky M. Oelze.

Writing – review & editing: Eden Washburn, Jason Nesbitt, Bebel Ibarra, Lars Fehren-Schmitz, Vicky M. Oelze.

References

1. Altschul J.H., Kintigh K.W., Aldenderfer M., Alonzi E., Armit I., Barceló J.A., et al. 2020. Opinion: To understand how migrations affect human securities, look to the past, Proceedings of the National Academy of Sciences 117, 20342–20345.
2. Bentley RA, Krause R, Price TD, Kaufmann B. Human mobility at the early Neolithic settlement of Vaihingen, Germany: evidence from strontium isotope analysis. Archaeometry. 2003; 45(3):471–86.
3. Blank M, Sjögren K-G, Knipper C, Frei KM, Storå J. Isotope values of the bioavailable strontium in inland southwestern Sweden—A baseline for mobility studies. PloS one. 2018; 13(10).
4. Eckardt H, Chenery C, Booth P, Evans J, Lamb A, Müldner G. Oxygen and strontium isotope evidence for mobility in Roman Winchester. Journal of Archaeological Science. 2009; 36(12):2816–25.
5. Frei KM, Price D. Strontium isotopes and human mobility in prehistoric Denmark. Archaeological and anthropological sciences. 2012; 4(2):103–14.
6. Gregoricka LA. Residential mobility and social identity in the periphery: strontium isotope analysis of archaeological tooth enamel from southeastern Arabia. Journal of Archaeological Science. 2013; 40 (1):452–64.
7. Lugli F, Cipriani A, Capecchi G, Ricci S, Boschin F, Boscato P, et al. Strontium and stable isotope evidence of human mobility strategies across the Last Glacial Maximum in southern Italy. Nature ecology & evolution. 2019; 3(6):905–11. https://doi.org/10.1038/s41559-019-0900-8 PMID: 31086279
8. Meijer J, Dolphin AE, Yakymchuk C, Gervers M. Interpreting medieval mobility from burials at the rock-hewn church of St. Georges, Gurat (France): Insights from strontium isotope analysis of bones and teeth. International Journal of Osteoarchaeology. 2019; 29(4):574–83.
9. Panagiotopoulou E, Montgomery J, Nowell G, Peterkin J, Doulgeri-Intzesiloglou A, Arachoviti P, et al. Detecting Mobility in Early Iron Age Thessaly by Strontium Isotope Analysis. European Journal of Archaeology. 2018; 21(4):590–611.
10. Shaw H, Montgomery J, Redfern R, Gowland R, Evans J. Identifying migrants in Roman London using lead and strontium stable isotopes. Journal of Archaeological Science. 2016; 66:57–68.
11. Sjögren K-G, Price TD, Ahlström T. Megaliths and mobility in south-western Sweden. Investigating relationships between a local society and its neighbours using strontium isotopes. Journal of anthropological archaeology. 2009; 28(1):85–101.
12. Ericson JE. Strontium isotope characterization in the study of prehistoric human ecology. Journal of Human Evolution. 1985; 14(5):503–14.
13. Faure G, Powell JL. Strontium isotope geology. New York.: Springer-Verlag; 1972.
14. Moore MJSaK. Bone Stable Isotope Studies in Archaeology. Journal of World Prehistory. 1992; 6(2).
15. Price TD, Burton JH, Bentley RA. The characterization of biologically available strontium isotope ratios for the study of prehistoric migration. Archaeometry. 2002; 44(1):117–35.
16. Slovak NM, Paytan A. Applications of Sr isotopes in archaeology. Handbook of environmental isotope geochemistry: Springer; 2012. p. 743–68.
17. Andrushko VA, Buzon MR, Simonetti A, Creaser RA. Strontium isotope evidence for prehistoric migration at Chokepukio, Valley of Cuzco, Peru. Latin American Antiquity. 2009:57–75.
18. Bethard JD, Gaither C, Sánchez VFV, Tham TER, Kent JD. Isótopos estables, dieta y movilidad de los pobladores de un conjunto residencial en Santa Rita B, Valle de Chao, Perú. Archaeobios. 2008;(2):3.
19. Barberena R, Durán VA, Novellino P, Winocur D, Benítez A, Tessone A, et al. Scale of human mobility in the southern Andes (Argentina and Chile): A new framework based on strontium isotopes. American journal of physical anthropology. 2017; 164(2):305–20. https://doi.org/10.1002/ajpa.23270 PMID: 28631376
20. Buzon MR, Conlee CA, Simonetti A, Bowen GJ. The consequences of Wari contact in the Nasca region during the Middle Horizon: archaeological, skeletal, and isotopic evidence. Journal of Archaeological Science. 2012; 39(8):2627–36.
21. Chala-Aldana D, Bocherens H, Miller C, Moore K, Hodgins G, Rademaker K. Investigating mobility and highland occupation strategies during the Early Holocene at the Cuncaicha rock shelter through strontium and oxygen isotopes. Journal of Archaeological Science: Reports. 2018; 19:811–27.

22. Conlee CA, Buzon MR, Gutierrez AN, Simonetti A, Creaser RA. Identifying foreigners versus locals in a burial population from Nasca, Peru: an investigation using strontium isotope analysis. Journal of Archaeological Science. 2009; 36(12):2755–64.

23. Durán VA, Cortegoso V, Barberena R, Frigolé C, Novellino P, Lucero G, et al. 'To and fro'the southern Andean highlands (Argentina and Chile): Archaeometric insights on geographic vectors of mobility. Journal of Archaeological Science: Reports. 2018; 18:668–78.

24. Hewitt BR. Foreigners among the dead at Túcume, Peru: Assessing residential mobility using isotopic tracers [PhD Dissertation]. Ontario: University of Western Ontario 2013.

25. Juengst SL. 3 Inclusive Communities In The Titicaca Basin During The Early Horizon. Archeological Papers of the American Anthropological Association. 2017; 28(1):24–37.

26. Juengst S, Chávez S, Hutchinson D, Mohr Chávez K. Trauma in the Titicaca Basin, Bolivia (AD 1000–1450). International Journal of Osteoarchaeology. 2015; 27(1):67–75.

27. Knudson KJ, Buikstra JE. Residential mobility and resource use in the Chiribaya polity of southern Peru: strontium isotope analysis of archaeological tooth enamel and bone. International Journal of Osteoarchaeology. 2007; 17(6):563–80.

28. Knudson KJ. Tiwanaku influence in the south central Andes: strontium isotope analysis and Middle Horizon migration. Latin American Antiquity. 2008:3–23.

29. Knudson KJ, Gardella KR, Yaeger J. Provisioning Inka feasts at Tiwanaku, Bolivia: the geographic origins of camelids in the Pumapunku complex. Journal of Archaeological Science. 2012; 39(2):479–91.

30. Knudson KJ, Giersz M, Więckowski W, Tomczyk W. Reconstructing the lives of Wari elites: Paleomobility and paleodiet at the archaeological site of Castillo de Huarmey, Peru. Journal of Archaeological Science: Reports. 2017; 13:249–64.

31. Knudson K, Price D, Buikstra J, Blom D. The use of strontium isotope analysis to investigate Tiwanaku migration and mortuary ritual in Bolivia and Peru. Archaeometry. 2004; 46(1):5–18.

32. Knudson KJ, Price TD. Utility of multiple chemical techniques in archaeological residential mobility studies: Case studies from Tiwanaku-and Chiribaya-affiliated sites in the Andes. American Journal of Physical Anthropology: The Official Publication of the American Association of Physical Anthropologists. 2007; 132(1):25–39. https://doi.org/10.1002/ajpa.20480 PMID: 17063464

33. Knudson KJ, Stanish C, Cerna MCL, Faull KF, Tantaleán H. Intra-individual variability and strontium isotope measurements: A methodological study using 87Sr/86Sr data from Pampa de los Gentiles, Chincha Valley, Peru. Journal of Archaeological Science: Reports. 2016; 5:590–7.

34. Knudson KJ, Torres-Rouff C. Cultural diversity and paleomobility in the Andean Middle Horizon: radiogenic strontium isotope analyses in the San Pedro de Atacama oases of Northern Chile. Latin American Antiquity. 2014; 25(2):170–88.

35. Knudson KJ, Tung TA, Nystrom KC, Price TD, Fullagar PD. The origin of the Juch'uypampa Cave mummies: strontium isotope analysis of archaeological human remains from Bolivia. Journal of Archaeological Science. 2005; 32(6):903–13.

36. Knudson KJ, Tung TA. Using archaeological chemistry to investigate the geographic origins of trophy heads in the central Andes: strontium isotope analysis at the Wari site of Conchopata. ACS Publications; 2007.

37. Knudson KJ, Torres-Rouff C. Investigating cultural heterogeneity in San Pedro de Atacama, northern Chile through biogeochemistry and bioarchaeology. American Journal of Physical Anthropology. The Official Publication of the American Association of Physical Anthropologists. 2009; 138(4):473–85.

38. Knudson KJ, Williams SR, Osborn R, Forgey K, Williams PR. The geographic origins of Nasca trophy heads using strontium, oxygen, and carbon isotope data. Journal of Anthropological Archaeology. 2009; 28(2):244–57.

39. Tung TA, Knudson KJ. Identifying locals, migrants, and captives in the Wari Heartland: A bioarchaeological and biogeochemical study of human remains from Conchopata, Peru. Journal of Anthropological Archaeology. 2011; 30(3):247–61.

40. Kurin DS, Lofaro E, Gómez Choque D, Krigbaum J. A bioarchaeological and biogeochemical study of warfare and mobility in Andahuaylas, Peru (ca. AD 1160–1260). International Journal of Osteoarchaeology. 2016; 26(1):93–103.

41. Marsteller SJ, Knudson KJ, Gordon G, Anbar A. Biogeochemical reconstructions of life histories as a method to assess regional interactions: Stable oxygen and radiogenic strontium isotopes and Late Intermediate Period mobility on the Central Peruvian Coast. Journal of Archaeological Science: Reports. 2017; 13:535–46.

42. Scaffidi BK, Knudson KJ. An archaeological strontium isoscape for the prehistoric andes: Understanding population mobility through a geostatistical meta-analysis of archaeological 87Sr/86Sr values from humans, animals, and artifacts. Journal of Archaeological Science. 2020; 117:105121.

43. Slovak NM, Paytan A, Wiegand BA. Reconstructing Middle Horizon mobility patterns on the coast of Peru through strontium isotope analysis. Journal of Archaeological Science. 2009; 36(1):157–65.

44. Slovak NM, Paytan A, Rick JW, Chien C-T. Establishing radiogenic strontium isotope signatures for Chavín de Huántar, Peru. Journal of Archaeological Science: Reports. 2018; 19:411–9.

45. Standen VG, Santoro CM, Arriaza B, Coleman D. Hunting, gathering, and fishing on the coast of the Atacama Desert: Chinchorro population mobility patterns inferred from strontium Isotopes. Geoarchaeology. 2018; 33(2):162–76.

46. Stanish C, Tantaleán H, Knudson K. Feasting and the evolution of cooperative social organizations circa 2300 BP in Paracas culture, southern Peru. Proceedings of the National Academy of Sciences. 2018; 115(29):E6716–E21.

47. Takigami M, Uzawa K, Seki Y, Chocano DM, Yoneda M. Isotopic Evidence for Camelid Husbandry During the Formative Period at the Pacopampa Site, Peru. Environmental Archaeology. 2019:1–17.

48. Thornton EK, Defrance SD, Krigbaum J, Williams PR. Isotopic evidence for Middle Horizon to 16th century camelid herding in the Osmore Valley, Peru. International Journal of Osteoarchaeology. 2011; 21(5):544–67.

49. Tomczyk W, Giersz M, Sołtysiak A, Kamenov G, Krigbaum J. Patterns of camelid management in Wari Empire reconstructed using multiple stable isotope analysis: evidence from Castillo de Huarmey, northern coast of Peru. Archaeological and Anthropological Sciences. 2019; 11(4):1307–24.

50. Tung TA, Knudson KJ. Social identities and geographical origins of Wari trophy heads from Conchopata, Peru. Current Anthropology. 2008; 49(5):915–25.

51. Turner BL, Kamenov GD, Kingston JD, Armelagos GJ. Insights into immigration and social class at Machu Picchu, Peru based on oxygen, strontium, and lead isotopic analysis. Journal of archaeological science. 2009; 36(2):317–32.

52. Turner BL, Armelagos GJ. Diet, residential origin, and pathology at Machu Picchu, Peru. American journal of physical anthropology. 2012; 149(1):71–83. https://doi.org/10.1002/ajpa.22096 PMID: 22639369

53. Knudson KJ, Tung TA. Investigating regional mobility in the southern hinterland of the Wari Empire: biogeochemistry at the site of Beringa, Peru. American journal of physical anthropology. 2011; 145 (2):299–310. https://doi.org/10.1002/ajpa.21494 PMID: 21469073

54. Jordán TE, Isacks BL, Allmendinger RW, Brewer JA, Ramos VA, Ando CJ. Andean tectonics related to geometry of subducted Nazca plate. Geological Society of America Bulletin. 1983; 94(3):341–61.

55. Montgomery DR, Balco G, Willett SD. Climate, tectonics, and the morphology of the Andes. Geology. 2001; 29(7):579–82.

56. Moseley ME. The Incas and Their Ancestors: The Archaeology of Peru (Revised Edition). New York, NY: Thames and Hudson Inc.; 2001.

57. Lau G. An archaeology of Ancash: Stones, ruins and communities in Andean Peru: Routledge; 2016.

58. Faure G. Principles of isotope geology. New York.: John Wiley; 1986.

59. Bentley RA. Strontium isotopes from the earth to the archaeological skeleton: a review. Journal of archaeological method and theory. 2006; 13(3):135–87.

60. Faure G, Mensing TM. Isotopes: principles and applications. Hoboken, N.J.: Wiley; 2005.

61. Knudson KJ, Webb E, White C, Longstaffe FJ. Baseline data for Andean paleomobility research: a radiogenic strontium isotope study of modern Peruvian agricultural soils. Archaeological and Anthropological Sciences. 2014; 6(3):205–19.

62. Knudson KJ, Williams HM, Buikstra JE, Tomczak PD, Gordon GW, Anbar AD. Introducing δ88/86Sr analysis in archaeology: a demonstration of the utility of strontium isotope fractionation in paleodietary studies. Journal of Archaeological Science. 2010; 37(9):2352–64.

63. Graustein WC. 87 Sr/86 Sr ratios measure the sources and flow of strontium in terrestrial ecosystems. Stable isotopes in ecological research: Springer; 1989. p. 491–512.

64. Bentley RA, Price TD, Lning J, Gronenborn D, Wahl J, Fullagar P. Prehistoric migration in Europe: strontium isotope analysis of early Neolithic skeletons. Current Anthropology. 2002; 43(5):799–804.

65. Gill KK, King DT Jr, Zou H, Smith F. Sedimentary Facies Analysis and Strontium-Isotope Stratigraphy of the Hillbank and Yalbac Formations, Corozal Basin, Belize. 2018.

66. Caus E, Frijia G, Parente M, Robles-Salcedo R, Villalonga R. Constraining the age of the last marine sediments in the late Cretaceous of central south Pyrenees (NE Spain): Insights from larger benthic foraminifera and strontium isotope stratigraphy. Cretaceous Research. 2016; 57:402–13.

67. Fan T, Yu K, Zhao J, Jiang W, Xu S, Zhang Y, et al. Strontium isotope stratigraphy and paleomagnetic age constraints on the evolution history of coral reef islands, northern South China Sea. Geological Society of America Bulletin. 2019.

68. Hoogewerff J, Reimann C, Ueckermann H, Frei R, Frei K, van Aswegen T, et al., editors. A preliminary bioavailable strontium isotope soil map of Europe. EGU General Assembly Conference Abstracts; 2017.

69. Kuznetsov A, Semikhatov M, Gorokhov I. Strontium isotope stratigraphy: principles and state of the art. Stratigraphy and Geological Correlation. 2018; 26(4):367–86.

70. Robinson E, Paytan A, Chien C. Strontium isotope dates for the Oligocene Antigua Formation, Antigua, WI. Caribbean Journal of Earth Science. 2017; 50:11–8.

71. Bataille CP, Bowen GJ. Mapping 87Sr/86Sr variations in bedrock and water for large scale provenance studies. Chemical Geology. 2012; 304:39–52.

72. Crowley BE, Miller JH, Bataille CP. Strontium isotopes (87Sr/86Sr) in terrestrial ecological and palaeoecological research: empirical efforts and recent advances in continental-scale models. Biological Reviews. 2017; 92(1):43–59. https://doi.org/10.1111/brv.12217 PMID: 26392144

73. Fenner JN, Frost CD. Revisiting the strontium contribution of sea salt in the human diet Journal of Archaeological Science 2014; 44:99–103.

74. Kamenov GD, Brenner M, Tucker JL. Anthropogenic versus natural control on trace element and Sr–Nd–Pb isotope stratigraphy in peat sediments of southeast Florida (USA), ~ 1500 AD to present. Geochimica et Cosmochimica Acta. 2009; 73(12):3549–67.

75. Willmes M, Bataille CP, James HF, Moffat I, McMorrow L, Kinsley L, et al. Mapping of bioavailable strontium isotope ratios in France for archaeological provenance studies. Applied Geochemistry. 2018; 90:75–86.

76. Elias RW, Hirao Y, Patterson CC. The circumvention of the natural biopurification of calcium along nutrient pathways by atmospheric inputs of industrial lead. Geochimica et Cosmochimica Acta. 1982; 46(12):2561–80.

77. Turekian KK, Kulp JL. The geochemistry of strontium. Geochimica et Cosmochimica Acta. 1956; 10 (5–6):245–96.

78. Rogers G, Hawkesworth CJ. A geochemical traverse across the North Chilean Andes: evidence for crust generation from the mantle wedge. Earth and Planetary Science Letters. 1989; 91(3–4):271–85.

79. Sillen A, Kavanagh M. Strontium and paleodietary research: a review. American Journal of Physical Anthropology. 1982; 25(S3):67–90.

80. Valentine B, Kamenov GD, Krigbaum J. Reconstructing Neolithic groups in Sarawak, Malaysia through lead and strontium isotope analysis. Journal of Archaeological Science. 2008; 35(6):1463–73.

81. Frei R, Frei KM. The geographic distribution of Sr isotopes from surface waters and soil extracts over the island of Bornholm (Denmark)–A base for provenance studies in archaeology and agriculture. Applied Geochemistry. 2013; 38:147–60.

82. Shand P, Darbyshire D, Love A, Edmunds W. Sr isotopes in natural waters: Applications to source characterisation and water–rock interaction in contrasting landscapes. Applied Geochemistry. 2009; 24(4):574–86.

83. Oelze VM, Koch JK, Kupke K, Nehlich O, Zäuner S, Wahl J, et al. Multi-isotopic analysis reveals individual mobility and diet at the early Iron Age monumental tumulus of Magdalenenberg, Germany. American Journal of Physical Anthropology. 2012; 148(3):406–21. https://doi.org/10.1002/ajpa.22063 PMID: 22553183

84. Buzon MR, Simonetti A, Creaser RA. Migration in the Nile Valley during the New Kingdom period: a preliminary strontium isotope study. Journal of Archaeological Science. 2007; 34(9):1391–401.

85. Montgomery J, Evans JA, Powlesland D, Roberts CA. Continuity or colonization in Anglo-Saxon England? Isotope evidence for mobility, subsistence practice, and status at West Heslerton. American Journal of Physical Anthropology: The Official Publication of the American Association of Physical Anthropologists. 2005; 126(2):123–38. https://doi.org/10.1002/ajpa.20111 PMID: 15386290

86. Giblin JI. Strontium isotope analysis of Neolithic and Copper Age populations on the Great Hungarian Plain. Journal of archaeological science. 2009; 36(2):491–7.

87. Kinaston RL, Walter RK, Jacomb C, Brooks E, Tayles N, Halcrow SE, et al. The first New Zealanders: patterns of diet and mobility revealed through isotope analysis. PloS one. 2013; 8(5).

88. Vésteinsson O, Gestsdóttir H. The colonization of Iceland in light of isotope analyses. Journal of the North Atlantic. 2014; 2014(sp7):137–45.

89. Grupe G, Price TD, Schröter P, Söllner F, Johnson CM, Beard BL. Mobility of Bell Beaker people revealed by strontium isotope ratios of tooth and bone: a study of southern Bavarian skeletal remains. Applied Geochemistry. 1997; 12(4):517–25.

90. Nelson BK, Deniro MJ, Schoeninger MJ, De Paolo DJ, Hare PE. Effects of diagenesis on strontium, carbon, nitrogen and oxygen concentration and isotopic composition of bone. Geochimica et Cosmochimica Acta. 1986; 50(9):1941–9.

91. Price TD, Johnson CM, Ezzo JA, Ericson J, Burton JH. Residential Mobility in the Prehistoric Southwest United States: A Preliminary Study using Strontium Isotope Analysis. Journal of Archaeological Science. 1994; 21:315–30.

92. Price TD, Knipper C, Grupe G, Smrcka V. Strontium isotopes and prehistoric human migration: the Bell Beaker period in central Europe. European journal of archaeology. 2004; 7(1):9–40.

93. Price TD, Manzanilla L, Middleton WD. Immigration and the ancient city of Teotihuacan in Mexico: a study using strontium isotope ratios in human bone and teeth. Journal of Archaeological Science. 2000; 27(10):903–13.

94. Price TD, Wahl J, Bentley RA. Isotopic evidence for mobility and group organization among Neolithic farmers at Talheim, Germany, 5000 BC. European Journal of Archaeology. 2006; 9(2–3):259–84.

95. Price TD, Tiesler V, Burton JH. Early African diaspora in colonial Campeche, Mexico: strontium isotopic evidence. American Journal of Physical Anthropology: The Official Publication of the American Association of Physical Anthropologists. 2006; 130(4):485–90. https://doi.org/10.1002/ajpa.20390 PMID: 16444728

96. Buzon MR, Simonetti A. Strontium isotope (87Sr/86Sr) variability in the Nile Valley: identifying residential mobility during ancient Egyptian and Nubian sociopolitical changes in the New Kingdom and Napatan periods. American Journal of Physical Anthropology. 2013; 151(1):1–9. https://doi.org/10.1002/ajpa.22235 PMID: 23440634

97. Eerkens JW, Carlson T, Malhi RS, Blake J, Bartelink EJ, Barfod GH, et al. Isotopic and genetic analyses of a mass grave in central California: Implications for precontact hunter-gatherer warfare. American journal of physical anthropology. 2016; 159(1):116–25. https://doi.org/10.1002/ajpa.22843 PMID: 26331533

98. Bentley RA, Price TD, Stephan E. Determining the 'local'87Sr/86Sr range for archaeological skeletons: a case study from Neolithic Europe. Journal of Archaeological Science. 2004; 31(4):365–75.

99. Grimstead DN, Nugent S, Whipple J. Why a standardization of strontium isotope baseline environmental data is needed and recommendations for methodology. Advances in Archaeological Practice. 2017; 5(2):184–95.

100. Knudson KJ, Price TD, Buikstra JE, Blom DE. The use of strontium isotope analysis to investigate Tiwanaku migration and mortuary ritual in Bolivia and Peru. Archaeometry. 2004; 46(1):5–18.

101. Ladegaard-Pedersen P, Achilleos M, Dörflinger G, Frei R, Kristiansen K, Frei KM. A strontium isotope baseline of Cyprus. Assessing the use of soil leachates, plants, groundwater and surface water as proxies for the local range of bioavailable strontium isotope composition. Science of The Total Environment. 2020; 708:134714. https://doi.org/10.1016/j.scitotenv.2019.134714 PMID: 31787293

102. West JB, Sobek A, Ehleringer JR. A simplified GIS approach to modeling global leaf water isoscapes. PloS one. 2008; 3(6). https://doi.org/10.1371/journal.pone.0002447 PMID: 18560592

103. Bowen GJ, West JB, Dawson TE. Isoscapes in a rapidly changing and increasingly interconnected world. Isoscapes: Springer; 2010. p. 425–32.

104. Bowen GJ. Isoscapes: spatial pattern in isotopic biogeochemistry. Annual Review of Earth and Planetary Sciences. 2010; 38:161–87.

105. Ehleringer JR, Thompson AH, Podlesak DW, Bowen GJ, Chesson LA, Cerling TE, et al. A framework for the incorporation of isotopes and isoscapes in geospatial forensic investigations. Isoscapes: Springer; 2010. p. 357–87.

106. Adams S, Grün R, McGahan D, Zhao JX, Feng Y, Nguyen A, et al. A strontium isoscape of north-east Australia for human provenance and repatriation. Geoarchaeology. 2019; 34(3):231–51.

107. Bataille CP, Von Holstein IC, Laffoon JE, Willmes M, Liu X-M, Davies GR. A bioavailable strontium isoscape for Western Europe: A machine learning approach. PloS one. 2018; 13(5). https://doi.org/10.1371/journal.pone.0197386 PMID: 29847595

108. Copeland SR, Cawthra HC, Fisher EC, Lee-Thorp JA, Cowling RM, Le Roux PJ, et al. Strontium isotope investigation of ungulate movement patterns on the Pleistocene Paleo-Agulhas plain of the Greater Cape floristic region, South Africa. Quaternary Science Reviews. 2016; 141:65–84.

109. Laffoon JE, Sonnemann TF, Shafie T, Hofman CL, Brandes U, Davies GR. Investigating human geographic origins using dual-isotope (87Sr/86Sr, δ18O) assignment approaches. PloS one. 2017; 12(2). https://doi.org/10.1371/journal.pone.0172562 PMID: 28222163

110. Meiggs DC, Arbuckle BS, Öztan A. The pixelated shepherd: Identifying detailed local land-use practices at Chalcolithic Köşk Höyük, central Turkey, using a strontium isotope (87Sr/86Sr) isoscape. Isotopic investigations of pastoralism in prehistory: Routledge; 2017. p. 77–95.

111. Pellegrini M, Pouncett J, Jay M, Pearson MP, Richards MP. Tooth enamel oxygen "isoscapes" show a high degree of human mobility in prehistoric Britain. Scientific reports. 2016; 6:34986. https://doi.org/10.1038/srep34986 PMID: 27713538

112. Francis P, Moorbath S, Thorpe R. Strontium isotope data for recent andesites in Ecuador and North Chile. Earth and Planetary Science Letters. 1977; 37(2):197–202.

113. Knudson KJ, Goldstein PS, Dahlstedt A, Somerville A, Schoeninger MJ. Paleomobility in the Tiwanaku diaspora: biogeochemical analyses at Rio Muerto, Moquegua, Peru. American journal of physical anthropology. 2014; 155(3):405–21. https://doi.org/10.1002/ajpa.22584 PMID: 25066931

114. Nesbitt J, Asencios BI, Tokanai F. The Architecture and Chronology of Reparin, Eastern Ancash, Peru. Ñawpa Pacha. 2020:1–19.

115. Ibarra B. Historia Prehispánica de Huari: Desde Chavín hasta los Inkas 3000 años de Historia: Lulu. com; 2009.

116. Ibarra B. Arqueología del Valle del Puchca: economía, cosmovisión y secuencia estilística. Arqueología de la sierra de Ancash: propuestas y perspectivas. 2003:251–330.

117. Ibarra B. Excavaciones en los sitios de Llamacorral y Marcajirca en el valle del Puccha, Provincia de Huari-Ancash. Informe Temporada. 2006.

118. Ibarra Ascencios B. A Diachronic Study of Mortuary Variablity in the North Highlands of Peru (AD 200–1600): Implications for understanding funeral practices and ancestor veneration. New Orleans, LA: Tulane University 2020.

119. Burger RL. Chavin de Huantar and its sphere of influence.] The Handbook of South American Archaeology: Springer; 2008. p. 681–703.

120. Burger RL. Chavin and the origins of Andean civilization. New York: Thames and Hudson; 1992. 248 p.

121. Lumbreras LG. Chavín de Huántar: excavaciones en la Galería de las Ofrendas: Von Zabern; 1993.

122. Rick JW. The evolution of authority and power at Chavín de Huántar, Peru. Archeological Papers of the American Anthropological Association. 2004; 14(1):71–89.

123. Rick JW. Context, construction, and ritual in the development of authority at Chavín de Huántar. Chavín: Art, architecture and culture. 2008:3–34.

124. Rick JW. Architecture and ritual space at Chavín de Huántar. Fux P, editor. Zurich: Museum Rietberg; 2013.

125. Tello JC. Discovery of the Chavin culture in Peru. American Antiquity. 1943; 9(1):135–60.

126. Tello JC. Chavín, cultura matriz de la civilización andina: la Universidad de San Marcos; 1960.

127. Cobbing J. Granites—An overview. Episodes-Newsmagazine of the International Union of Geological Sciences. 1996; 19(4):103–6.

128. Cobbing EJ, EJ C, WS P, JJ W, JW B. The geology of the Western Cordillera of northern Peru. 1981.

129. INGEMMET. Instituto Geológico Minero and y Metalúrgico. 1999.

130. Jacay J, Jaillard E, Marocco R. Latest Cretaceous to Paleocene red beds of Peru, and the early stages of the Andean deformation. 1996.

131. Evans JA, Montgomery J, Wildman G, Boulton N. Spatial variations in biosphere 87Sr/86Sr in Britain. Journal of the Geological Society. 2010; 167(1):1–4.

132. Snoeck C, Ryan S, Pouncett J, Pellegrini M, Claeys P, Wainwright AN, et al. Towards a biologically available strontium isotope baseline for Ireland. Science of The Total Environment. 2020; 712:136248. https://doi.org/10.1016/j.scitotenv.2019.136248 PMID: 31945525

133. Rosenthal G, Nelson D, Gardiner D. Deposition of strontium and calcium in snail shell. Nature. 1965; 207(4992):51–4. https://doi.org/10.1038/207051b0 PMID: 5866525

134. Murra JV. El" control vertical" de un máximo de pisos ecológicos en la economía de las sociedades andinas. 1972.

135. Forman SH. The future value of the" verticality" concept: Implications and possible applications in the Andes 1976.

136. Maxwell K. Beyond verticality: fuelscape politics and practices in the Andes. Human Ecology. 2011; 39 (4):465–78.

137. Paerregaard K. Complementarity and duality: Oppositions between agriculturists and herders in an Andean village. Ethnology. 1992; 31(1):15–26.

138. Sanchez R. The Model of Verticality in the Andean Economy: A Critical Reconsideration. Bulletin of the Society for Latin American Studies. 1977;(27):24–49.

139. Stanish C. Ancient Andean political economy: University of Texas Press; 1992.

140. Finucane B, Agurto PM, Isbell WH. Human and animal diet at Conchopata, Peru: stable isotope evidence for maize agriculture and animal management practices during the Middle Horizon. Journal of Archaeological Science. 2006; 33(12):1766–76.

141. Finucane BC. Mummies, maize, and manure: multi-tissue stable isotope analysis of late prehistoric human remains from the Ayacucho Valley, Peru. 2007; 34(12):2115–24.

142. Finucane BC. Maize and sociopolitical complexity in the Ayacucho Valley, Peru. Current Anthropology. 2009; 50(4):535–45.

143. Sutter RC. Prehistoric genetic and culture change: a bioarchaeological search for pre-Inka altiplano colonies in the coastal valleys of Moquegua, Peru, and Azapa, Chile. Latin American Antiquity. 2000:43–70.

144. White CD, Nelson AJ, Longstaffe FJ, Grupe G, Jung A. Landscape bioarchaeology at Pacatnamu, Peru: inferring mobility from δ 13 C and δ 15 N values of hair. Journal of Archaeological Science. 2009; 36(7):1527–37.

145. Brush SB. Man's use of an Andean ecosystem. Human Ecology. 1976; 4(2):147–66.

146. Moseley ME. The exploration and explanation of early monumental architecture in the Andes. Early ceremonial architecture in the Andes. 1985:29–58.

147. Hirsch E. Remapping the Vertical Archipelago: Mobility, Migration, and the Everyday Labor of Andean Development. The Journal of Latin American and Caribbean Anthropology. 2018; 23(1):189–208.

148. Murra JV. The limits and limitations of the 'vertical archipelago'in the Andes. Andean ecology and civilization: An interdisciplinary perspective on Andean ecological complementarity. 1985; 91:15.

149. Van Buren M. Rethinking the vertical archipelago: ethnicity, exchange, and history in the south central Andes. American Anthropologist. 1996:338–51.

150. Tomczak PD. Prehistoric diet and socioeconomic relationships within the Osmore Valley of southern Peru. Journal of Anthropological Archaeology. 2003; 22(3):262–78.

151. Evans J, Pearson MP, Madgwick R, Sloane H, Albarella U. Strontium and oxygen isotope evidence for the origin and movement of cattle at Late Neolithic Durrington Walls, UK. Archaeological and Anthropological Sciences. 2019; 11(10):5181–97.